ORGANISMAL BIOLOGY

A heritable subset of the core rumen microbiome dictates dairy cow productivity and emissions

R. John Wallace[1]*[†], Goor Sasson[2][†], Philip C. Garnsworthy[3], Ilma Tapio[4], Emma Gregson[3], Paolo Bani[5], Pekka Huhtanen[6], Ali R. Bayat[4], Francesco Strozzi[7][‡], Filippo Biscarini[7][§], Timothy J. Snelling[1], Neil Saunders[3], Sarah L. Potterton[3], James Craigon[3], Andrea Minuti[5], Erminio Trevisi[5], Maria L. Callegari[8][||], Fiorenzo Piccioli Cappelli[5], Edward H. Cabezas-Garcia[6][¶], Johanna Vilkki[4], Cesar Pinares-Patino[4], Kateřina O. Fliegerová[9], Jakub Mrázek[9], Hana Sechovcová[9], Jan Kopečný[9], Aurélie Bonin[10], Frédéric Boyer[10], Pierre Taberlet[10], Fotini Kokou[2], Eran Halperin[11], John L. Williams[7][#]**, Kevin J. Shingfield[4]**[††], Itzhak Mizrahi[2]***

A 1000-cow study across four European countries was undertaken to understand to what extent ruminant microbiomes can be controlled by the host animal and to identify characteristics of the host rumen microbiome axis that determine productivity and methane emissions. A core rumen microbiome, phylogenetically linked and with a preserved hierarchical structure, was identified. A 39-member subset of the core formed hubs in co-occurrence networks linking microbiome structure to host genetics and phenotype (methane emissions, rumen and blood metabolites, and milk production efficiency). These phenotypes can be predicted from the core microbiome using machine learning algorithms. The heritable core microbes, therefore, present primary targets for rumen manipulation toward sustainable and environmentally friendly agriculture.

INTRODUCTION

Hosting one of the most complex microbial communities known to man, the rumen has long attracted the keen interest of microbiologists. Physiologists and nutritionists also understand the pivotal role of the rumen in digesting fibrous feed and providing nutrients to the host animal. These activities enable ruminants to provide humans with foods, mainly milk and meat from nonhuman-edible plant material, including industrial by-products, and enable many rural communities worldwide to survive where arable agriculture is impossible. There is an environmental cost, however, in which ruminants, via their ruminal microbiome, produce substantial amounts of the greenhouse gas, methane (1). Furthermore, production effi-

ciency is linked to the composition of the ruminal microbiome, as was previously shown by an association between microbiome components and residual feed intake (2, 3). Characterizing, quantifying, and understanding the role of rumen microbiome are therefore of significant scientific, economic, and environmental interest.

The main members of the rumen microbiome are now well understood. Bacteria, which usually comprise most of the species richness, are widely persistent geographically across multiple ruminant species and individual animals (4), and many species can be considered symbiotic with ruminants, as they provide metabolic activities and products essential for the host (5). Ciliate protozoa, at up to about half the biomass, consist of species that occur uniquely in the rumen (6). Their community abundance and composition across ruminants are much more variable than bacteria, indeed, protozoa may be absent in some animals without detrimental effect to the host (4, 7). Anaerobic fungi are fewer in number but seem to play an important role in breaking down the toughest of plant cell walls (8). Archaea are key players in methane emissions (9).

Generally speaking, the relationship between members of the microbiome and rumen function is reasonably well understood (10). A host genetics microbiome axis of control has also been implied in several studies (11–13), analogous to, but much less detailed than the remarkable advances in our understanding of the role of the heritability of the human gut microbiome and its role in health (14). In the present study, by applying network analysis to a comprehensive array of microbiome, phenotype, and genotype analysis, we have made a significant contribution in transforming the descriptive understanding of the rumen microbiome to a predictive one, using an unprecedentedly large number of animals and measurements. It emerges, as suggested by an earlier, much more restricted study (15) that rumen function and ruminant productivity can be predicted from the abundance of a small number of microorganisms that form part of the core community across geographical breed and dietary differences. As these microbes show significant heritability estimates, e.g., their abundance is explained to a significant

[1]The Rowett Institute, University of Aberdeen, Ashgrove Road West, Aberdeen AB25 2ZD, UK. [2]Department of Life Sciences and the National Institute for Biotechnology in the Negev, Ben-Gurion University of the Negev, Be'er Sheva, Israel. [3]University of Nottingham, School of Biosciences, Sutton Bonington Campus, Loughborough LE12 5RD, UK. [4]Production Systems, Natural Resources Institute Finland (Luke), 31600 Jokioinen, Finland. [5]Department of Animal Science, Food and Nutrition-DIANA, Università Cattolica del Sacro Cuore, 29122 Piacenza, Italy. [6]Swedish University of Agricultural Sciences, Department of Agriculture for Northern Sweden, S-90 183 Umeå, Sweden. [7]Parco Tecnologico Padano, Via Einstein, 26900 Lodi, Italy. [8]Institute of Microbiology, Università Cattolica del Sacro Cuore, 29122 Piacenza, Italy. [9]Institute of Animal Physiology and Genetics, CAS, v.v.i., Vídeňská 1083, Prague 14220, Czech Republic. [10]Laboratoire d'Ecologie Alpine, Domaine Universitaire de St Martin d'Hères CNRS, 38041 Grenoble, France. [11]Departments of Computer Science, Computational Medicine, Human Genetics, and Anesthesiology, University of California, Los Angeles, Los Angeles, CA 90095, USA.
*Corresponding author. Email: john.wallace@abdn.ac.uk (R.J.W.); imizrahi@bgu.ac.il (I.M.)
†Joint first authors.
‡Present address: Enterome Bioscience 94/96 Avenue Ledru-Rollin, 75011 Paris, France.
§Present address: National Research Council, Institute of Biology and Biotechnology in Agriculture (CNR-IBBA), Via Bassini 15, 20133 Milan, Italy.
||Present address: Department for Sustainable Food Process –DiSTAS, Università Cattolica del Sacro Cuore, Via E.Parmense 84, 29122 Piacenza, Italy.
¶Present address: Agri-Food and Biosciences Institute, AFBI Large Park, Hillsborough BT26 6DR Co. Down, UK.
#Present address: Davies Research Centre, School of Animal and Veterinary Sciences, Faculty of Sciences, University of Adelaide, Roseworthy, SA 5371, Australia.
**Joint last authors.
††Deceased.

extent by host genetics, opportunities for breeding programs based on the microbiome now become possible.

RESULTS

Our study cohort consisted of 1016 animals, with 816 Holstein dairy cows from two U.K. and three Italian farms. In addition, 200 Nordic Red dairy cows were sampled from Sweden and Finland. The Holsteins received a maize silage–based diet, while the Nordic Reds received a nutritionally equivalent diet based on grass silage as forage. Animals were genotyped using common single-nucleotide polymorphisms (SNPs) and measured for milk output and composition, feed intake and digestibility, plasma components, methane and CO_2 emissions, and rumen microbiome based on ss rRNA gene analysis (data S1).

The abundance and richness of the bacterial, protozoal, fungal, and archaeal communities were mutually dependent on and correlated to multiple host phenotypes in ways that have become widely understood, including rumen metabolites, milk production indices, and plasma metabolites (see Supplementary Text and fig. S4). To focus down on host microbiome–phenotype relationships, we proceeded

to investigate (i) how many and which species were common in our large animal cohorts; (ii) if a common, or core, group could be identified; (iii) if the core was influenced by the host genome; and (iv) how the core and noncore species determined phenotypic and production characteristics.

Taxonomic analysis revealed a core group of rumen microbes [512 species-level microbial operation taxonomic units (OTUs), 454 prokaryotes, 12 protozoa, and 46 fungi] present in at least 50% of animals within each of the seven farms studied (Fig. 1A). The group comprised 11 prokaryotic orders, 1 fungal order, and 2 protozoal orders that share some similarity with published core microbial communities (data S2 to S4) (6, 15). The core group was shared between Holstein and Nordic Red dairy breeds, and the results are particularly useful because they apply to the most popular and productive milking cow breed used in developed countries, the Holstein, and the smaller breed used in northern European latitudes, the Nordic Red. The results demonstrate once again, however, that this microbial community is representative of ruminants in general, especially with respect to bacterial and protozoal species. This core community is significantly enriched in Bacteroidales, Spirochetales, and the WCHB1-41 order (Fig. 1B and data S5 to S7). The core
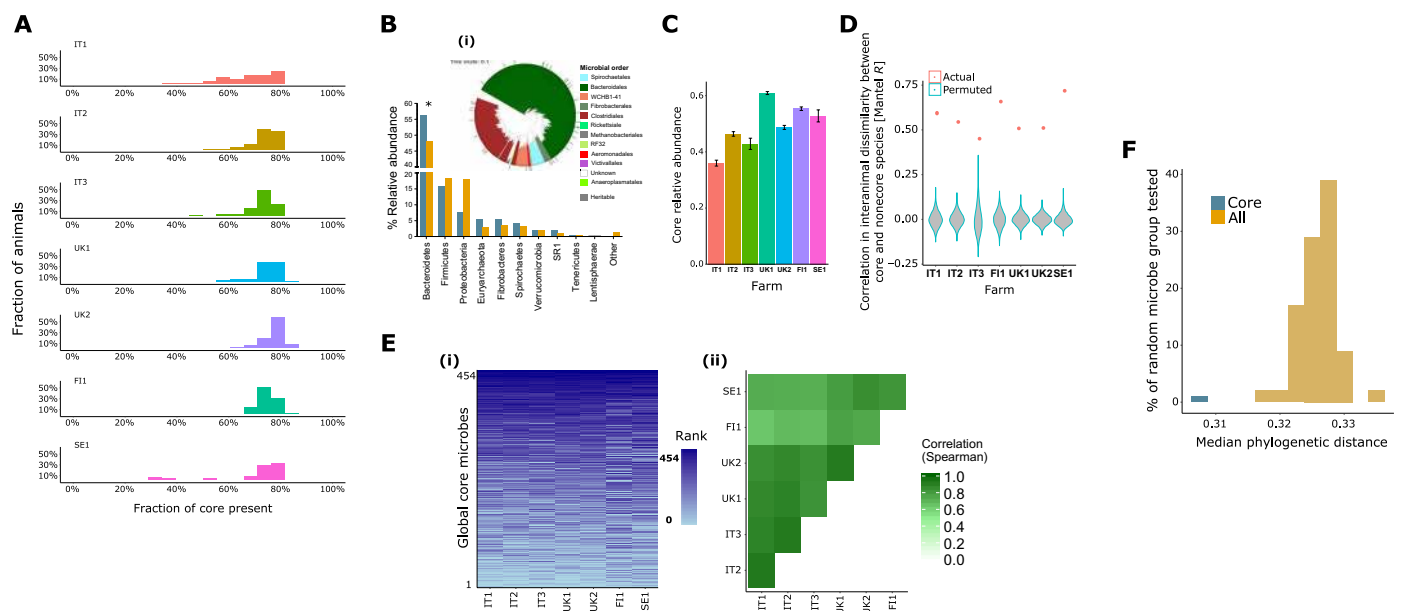
Fig. 1. A phylogenetically cohesive core rumen microbiome was found across farms with highly conserved hierarchical structure and tight association to overall microbiome composition. (**A**) Core microbes are highly represented within individual animals, as a high fraction of them (>50% of the core microbes) are present in >70% of the individuals. (**B**) The prokaryotic core (blue) was represented by 10 phyla of the 30 found in the overall microbiome (x axis; ochre), including 11 prokaryotic, 2 fungal, and 1 protozoal orders, detected in >50% of the individuals in each farm. *The core microbiome was significantly enriched in Bacteroidetes (enrichment analysis, Fisher exact test, after Benjamini-Hochberg correction, $P < 0.0005$). SR1, candidate division sulphur river 1. Core prokaryotes (i) consisted of 454 microbes, mainly from the orders Bacteroidales (tree; green) and Clostridiales (tree; maroon). Core heritable taxa are presented as gray bar plots on the tree. (**C**) The core microbiome composed of a large fraction of the overall microbiome, ranging between three- and two-thirds of the relative abundance, depending on the farm (x axis). Bar plots represent the mean, and error bars represent the SE of the core relative abundance. (**D**) Core microbiome composition is highly correlated to noncore microbes, as shown by comparing the interanimal dissimilarity (Bray-Curtis) matrix based on core microbes to that based on noncore microbes. Violin plots for each farm (x axis) show the correlation between the two dissimilarity matrices (core and noncore; Mantel R), where the violin (gray) describes the null model (permuted) Mantel R values, and red points depict the actual R. (**E**) The core microbiome exhibits a clear hierarchical structure, in terms of microbial abundance, which agrees between farms. (i) A highly consistent core microbiome abundance pattern (ranking) across farms (x axis) was revealed by an abundance-ranked color-coded heatmap, where species-level microbial OTUs are ordered by their mean relative abundance across all animals in the cohort (no further clustering or normalization was performed). Color coding reflects the rank abundance of a given OTU in a given individual. (ii) Heatmap showing the degree of correlation in relative abundance profiles between the farms. Color coding reflects the degree of correlation in relative abundance profiles (Spearman r; all $P < 0.001$). (**F**) Phylogenetic distances between the core microbes were smaller, showing that they are closer phylogenetically, but also distinct, compared to the overall microbiome, as it was shown by mean pairwise phylogenetic distance (x axis) calculation between core (blue) and 1000 randomly selected noncore microbes (ochre) from the rumen (y axis; $P < 0.001$).

microbiome consists of less than 0.25% of the overall microbial species pool (512 of 250,000 OTUs), yet it is highly abundant, representing 30 to 60% of the overall microbiome (Fig. 1C). The core group is also tightly associated with the overall microbiome, as reflected by high correlation between the beta diversity metrics of the identified core microbiome and the overall microbiome across farms (R value between 0.45 and 0.7; Fig. 1D), this strengthens the notion of strong connectivity between microbes in such a metabolically complex ecosystem where multiple microbial interactions are potentially facilitated. These core microbes show highly conserved abundance rank structure across geography, breed, and diet (Fig. 1E), where the species abundance order is kept almost identical across different individuals. Furthermore, core members are more closely related to each other than to noncore microbiome members, as indicated by differences in phylogenetic distances determined by the ss rRNA gene tree (Fig. 1F), thereby strengthening the findings from our previous study (15). Thus, this relatedness between the members of the rumen core microbiome could indicate that they are sharing a set of functional traits, integral to this environment and potentially compatible with host requirements as suggested for species relatedness in other ecosystems (16). Although the rumen microbiome contains many hundreds of species, these core species generally belong to a rather narrow section of the whole bacterial phylome (17).

We found the core microbiome to be significantly correlated with host genetics as revealed by canonical correlation analysis (CCA), which was calculated for each farm separately (Fig. 2A). Subsequently, a stringent heritability analysis was applied to all members of the core microbiome for each breed separately, taking into account farms and dietary components as a confounding effect (farm encompasses other confounding effects such as location and husbandry regime; see further explanation in Supplementary Materials and Methods). Moreover, we removed one Holstein farm (UK2) from the analysis as it showed a different genetic background (UK2; fig. S2). Our heritability analysis specifically quantifies narrow sense, unlike twin-based studies where the type of heritability is not strictly defined (14). This is especially true for bovines where the twin rate is low, and these individuals are often born unwell, rendering them unfit for these studies. Within the Holstein-Friesian breed ($n = 650$, excluding 166), 39 heritable core microbial OTUs were identified, which were evenly distributed on the rank abundance curve, therefore pointing out that low-abundance species could also be connected to host genome and suggesting relevance to its requirements (fig. S1). These not only mainly belong to Bacteroidales and Clostridiales orders but also include representatives from five other bacterial phyla and two fungi of the genus *Neocallimastix* (Fig. 2B and data S8 and S10). *Ruminococcus* and *Fibrobacter* are among the core heritable bacteria, consistent with their key role in cellulolysis, as is Succinovibrionaceae, which seems to be a key determinant in between animal differences in methane emissions (18). These heritable microbial OTUs showed significant heritability estimates ranging from 0.2 to 0.6 [false discovery rate (FDR), $P < 0.05$] and revealed a twofold increase in numbers of microbial heritable species in a previous study (15) that included a smaller animal cohort. Furthermore, these highly robust findings also reinforce our previous results in relation to heritable bovine rumen microbes, which are composed of similar taxa. Moreover, on the basis of the genetic relatedness matrix (GRM), the heritability confidence interval lower limit of all but one microbe was greater than 0.1. Only three bacteria, all with affiliations to Prevotellaceae, were identified as highly heritable within the smaller Nordic

Red cohort. In summary, we identified almost 10 times more heritable species-level microbial OTUs than in a comparable human study (14), further substantiating the deep interaction between the bovine host and its resident rumen microbiome, presumably reflecting the greater dependence of the bovine on its gut microbiome than humans.

Overall, when microbial co-occurrence networks were inferred within individual farms (fig. S3, A to D), it became evident that heritable microbes are significantly more connected than nonheritable microbes, consistent with the central positions of heritable microbes in the rumen co-occurrence networks (Fig. 2C).

The demonstration here of heritable, interacting microbes raises possibilities of breeding animals for particular microbiomes and thus phenotypic and production properties on the condition that the core can be shown to control these properties. We further investigated co-occurrence networks for the core abundances relation to phenotypic outcomes.

The associations found here are hugely complex (Fig. 3A), with not only 339 microbes, mostly prokaryotes, but also a handful of protozoa and fungi, associated with rumen metabolism and various host phenotypes (see also data S7). The resulting network (Fig. 3A) only included reoccurring significant correlations with the same directionality (FDR < 0.05) within at least four farms when analyzed independently. As would be expected from the nutritional dependence of ruminants on volatile fatty acids (VFA) generated by rumen fermentation, large numbers of core microbiome members were found to be associated with traits such as ruminal acetate and propionate concentration, with fewer correlated to production traits such as milk production and methane emission (204, 254, 23, and 7, respectively; Fig. 3B). Among those linked to methane emissions are Succinovibrionaceae, confirming what has been found previously in beef cattle (18). Compared to the overall rumen microbiome, prokaryotic members of the core microbiome are highly enriched with trait-associated microbes [odds ratio (OR), 388; $P < 2.2 \times 10^{-16}$, Fisher exact test between 332 trait-related and 454 prokaryotic core members; Fig. 3C], stressing the importance and central role that the core microbiome plays in host function and microbiome metabolism. Two distinctive machine learning algorithms were applied to predict rumen metabolism diet and host traits, based on core microbiome composition, Ridge regression (19, 20) and random forest (RF) (21, 22), using linear regression and decision tree–based approaches, respectively. This allowed us to investigate the degree of agreement (r^2) between predicted and actual values (Fig. 3D and fig. S5). These tools highlighted the core microbiome as highly explanatory for dietary components and rumen metabolites, with propionate approaching an agreement of $r^2 = 0.9$ in some farms. Methane emissions could also be explained, based on rumen microbiome composition, with values reaching $r^2 = 0.4$ in some farms. Moreover, although having lower explainability, many of the host traits, including host plasma metabolites and milk composition, could be explained to an extent by the core microbiome composition (Fig. 3D). Our findings also show that core microbiome has higher prediction power than host animals' genotype (based on the GRM), as has dietary composition (fig. S5). Overall, in both machine learning algorithms, the heritable microbes exhibited, on average, a significantly higher explanatory power for host phenotypes and other experimental variables compared to other core microbes ($P < 0.005$, Wilcoxon paired rank-sum test; figs. S6 and S7), further underlining the central role of heritable microbes within rumen microbial ecology and to the host. The great majority of these microbes show stability in
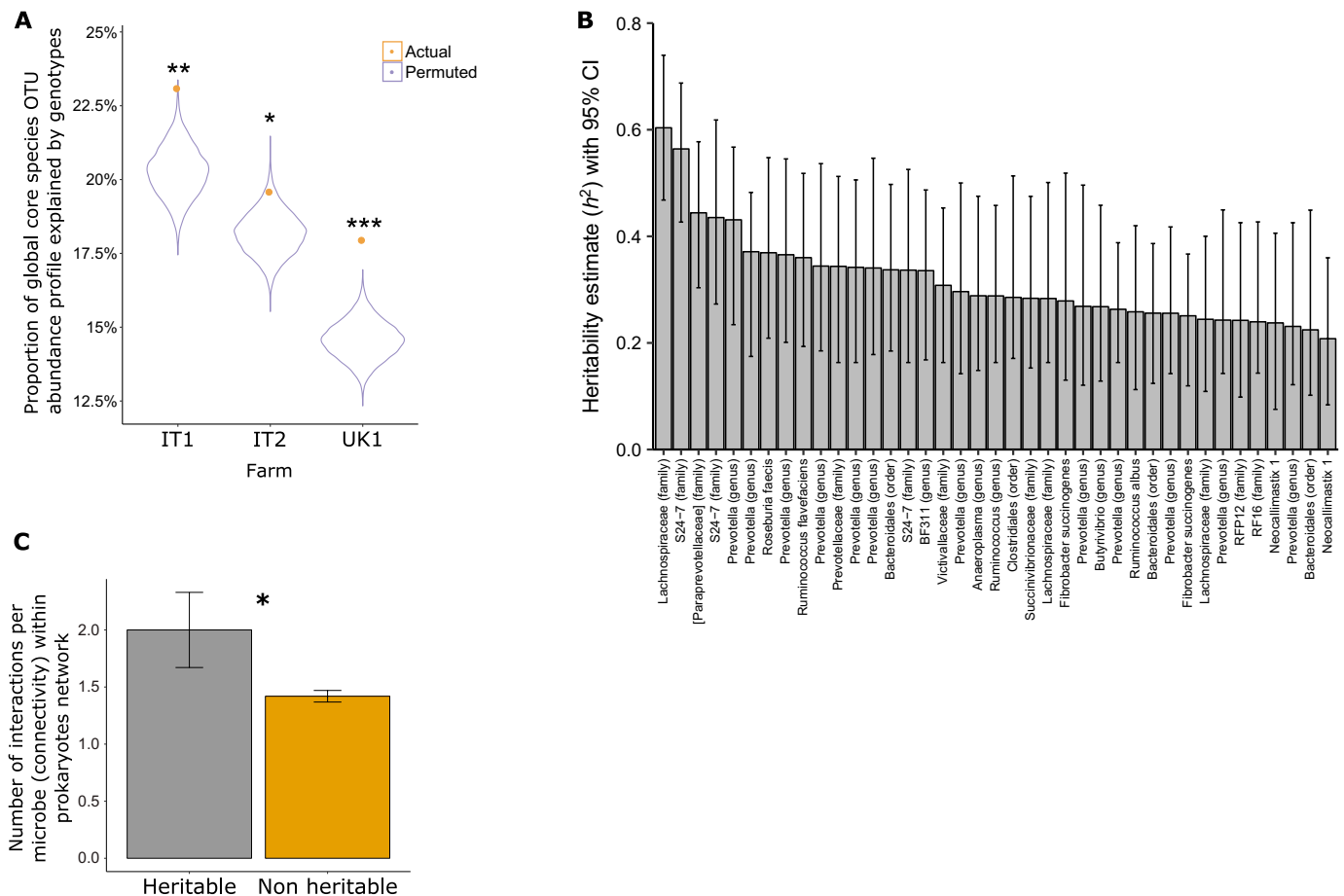
Fig. 2. Host genetics explains core microbiome composition with heritable microbes serving as hubs within the microbial interaction networks. The core microbiome is associated with animal genetics as (**A**) the variance in the core microbiome (y axis) was significantly explained by host genetics. CCA was performed between the matrix of the first 30 microbial (OTU table) principal component scores and host genotype principal component scores based on a common SNP. The analysis was accomplished for the largest Holstein farms in this study (x axis). (**B**) Heritability analysis based on the genetic relatedness matrix (GRM) showed 39 microbes (x axis) significantly correlating with the animal genotype. Heritability estimate—h^2 (y axis; bar plots show mean estimate per microbe), and P values were calculated using genetics complex trait analysis (GCTA) software, followed by a multiple testing correction with Benjamini-Hochberg method. Confidence intervals (CIs; 95%) were estimated on the basis of heritability estimates and the GRM with Fast Confidence IntErvals using Stochastic Approximation (FIESTA) software. (**C**) Heritable microbes are central to the microbial interaction network, as revealed by the higher mean connectivity (y axis) of these microbes compared to the nonheritable ones. The interaction network was built using Sparse InversE Covariance estimation for Ecological Association and Statistical Inference (SpiecEasi). Results are presented as mean number of microbial interactions with SE. Indicated P values, *$P < 0.05$, **$P < 0.005$, ***$P < 0.0005$.

time, and only a small portion of them (39, 3 heritable and 1 trait associated) showed seasonality, and of those, most do so solely in one of the farms (fig. S8 and data S9).

DISCUSSION AND CONCLUSIONS

Here, we have shown that a small number of host-determined, heritable microbes make higher contribution to explaining experimental variables and host phenotypes (fig. S6) and propose microbiome-led breeding/genetic programs to provide a sustainable solution to increase efficiency and lower emissions from ruminant livestock. On the basis of the genetic determinants of the heritable microbes, it should be possible to optimize their abundance through selective breeding programs. A different, and perhaps more immediate, application of our data could be to modify early-life colonization, a factor that has been shown to drive microbiome composition and activity in later life (23–25). Inoculating key core species associated

with feed efficiency or methane emissions as precision probiotics approach could be considered as likely to complement the heritable microbiome toward optimized rumen function.

Our study focused on two bovine dairy breeds, but the results are likely to be applicable to beef animals and other ruminant species. Given the high importance of diet in performance and the composition of the rumen microbiome, these programs should take special cognizance of likely feeding regimes. Within that context, following the overall predictive impact of identified trait-associated heritable microbes on production indices should result in a more efficient and more environmentally friendly ruminant livestock industry.

MATERIALS AND METHODS
Experimental design and subject details
The primary objective of this research was to relate the animal genome to the rumen microbiome, feed efficiency, and methane
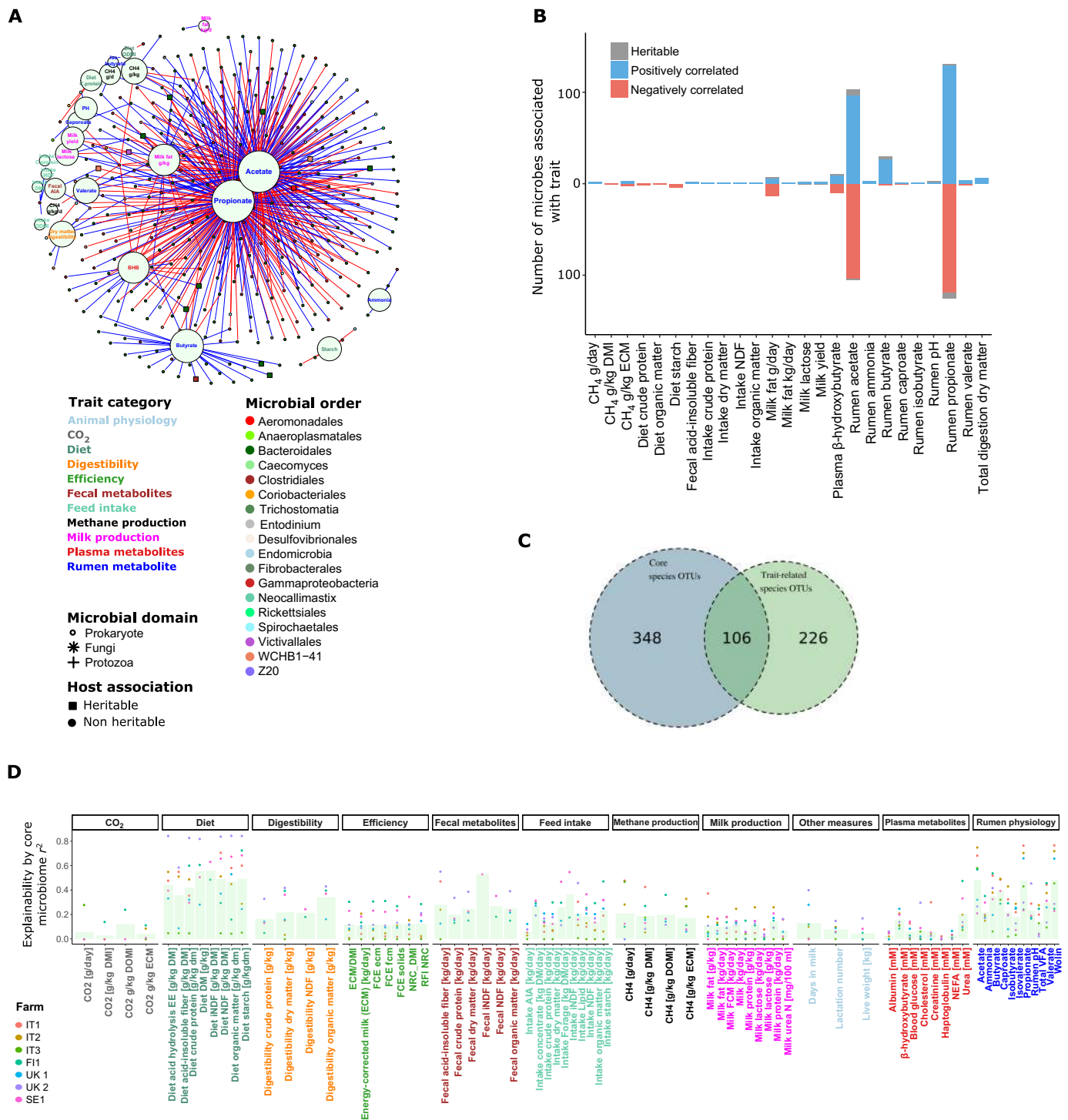
Fig. 3. Core rumen microbiome composition is linked to host traits and could significantly predict those traits. (**A**) Association analysis between microbes and host traits revealed 339 microbes associated with at least one trait. For a microbe to be associated with a given trait, it had to significantly and unidirectionally correlate with a trait within each of at least four farms (after Benjamini-Hochberg multiple testing correction) with no farm showing a significant correlation in the opposing direction. (**B**) Most of the trait-associated microbes are associated with rumen propionate and acetate. (**C**) Enrichment analysis, using Fisher exact test, showed that the core microbes are much more present (enriched) within trait-associated microbes compared to the noncore microbiome ($P < 2.2 \times 10^{-16}$). (**D**) Explained variation (r^2) of different host traits as function of core microbiome composition. r^2 estimates were derived from a machine learning approach where a trait value was predicted for a given animal using the Ridge regression that was constructed from other animals in the farm (leave-one-out k-fold regression). Thereafter, prediction r^2 value was calculated between the vectors of observed and predicted trait values. Indicated host traits were significantly explained (via prediction) by core microbe (OTU) abundance profiles. Dots stand for individual farms' prediction r^2, while bar heights represent mean of individual farms' r^2. DMI, dry matter intake; ECM, energy-corrected milk; NDF, neutral-detergent fiber; DM, dry matter; BHB, β-hydroxybutyrate.

emissions in lactating dairy cows. The following research questions were specified at the outset: Does host genetics have a significant effect on the overall microbiome composition and to what extent? How consistent is the rumen microbiome across geographic locations, breeds, and diets? On discovery of a heritable core rumen microbiome, the following additional research questions arose: Do heritable rumen microbes interact with the rest of the core rumen microbes? How do heritable microbes integrate in the overall microbe host phenotype interaction network?

The objectives were addressed in an observational study involving collection of phenotypic data describing animal metabolism, digestion efficiency, and emissions of methane and nitrogen. Samples of rumen digesta and blood were collected for molecular analysis and subsequent statistical analysis to identify correlations and genetic associations. Precise power calculations to determine the size of study population necessary were difficult, as for this new area of research, the size and architecture of the genetic effect were unknown. In addition, variations during life cycle, e.g., age and stage of lactation, together with nutrition environmental factors would play a role in overall variations. After considering levels of variation encountered in similar studies, we considered that, with 1000 individuals, using standardized measurements and keeping them under standardized conditions, it would certainly be possible to identify major genetic loci affecting the target traits from a genome-wide association study. The final population sampled was 1016 cows to allow a small margin in case any individuals or samples had to be excluded.

Prospective inclusion criteria for animal selection were that cows must be between 10 and 40 weeks postpartum, had received the standard diet for at least 14 days, and had no health issue in the current lactation. Prospective data exclusion criteria were missing samples (e.g., milk, blood, rumen, and feces), sample processing issues (e.g., inadequate DNA yield, assay problems, and laboratory mishaps), and implausible outliers. Statistical outliers were defined as values greater than three SDs from the mean. All statistical outliers were investigated, calculations were corrected, or assays were repeated where appropriate. Otherwise, outliers were retained for data analysis unless they were implausible. Data for any excluded sample were omitted, but the remaining data for the individual were retained.

Six milk samples were missing due to a faulty sampling device, and one blood sample was missing from a cow that could not be sampled. Two rumen fluid samples were lost during laboratory analysis. Two estimates of feed intake were considered implausible (200% of expected) due to abnormal fecal alkane values.

Animal work was conducted by four research teams in the United Kingdom (UK), Italy (IT), Sweden (SE), and Finland (FI). Ethical approval was granted by the relevant local and national authorities and committees before sampling commenced at each center (permit numbers: FI, ESAVI/8182/04.10.03/2012; IT, 25906/13; SE, A143-12; UK, 40/3324 and 30/3201). In total, 1016 cows on seven farms were sampled, and associated data were collected. The UK sampled 409 cows on two farms (UK1, $N = 243$; UK2, $N = 164$); IT sampled 409 cows on three farms (IT1, $N = 185$; IT2, $N = 176$; IT3, $N = 48$); SE sampled 100 cows on one farm (SE1); and FI sampled 100 cows on one farm (FI1).

Experimental protocols for measuring animal phenotypes were agreed before sampling commenced. Recordings and collection of biological samples were performed over a 5-day period for each cow that had received the standard diet for at least 14 days. To reach 1016 cows, sampling was conducted over a period of 26 months in 78 sessions between 1 and 40 cows per session. At time of recording

and sampling, all cows were in established lactation (between 10 and 40 weeks postpartum) when energy balance is close to zero and methane output is relatively stable (26). Implementation of methodology varied between centers due to facilities available on different farms. In each case, we chose the most accurate method appropriate for the circumstances while ensuring that methods produced comparable results across all farms.

Method details
Housing and feeding systems
Cows on all farms were group-housed in loose housing barns, except in FI where cows were housed in individual standings during the sampling period. To minimize environmental variation, all cows were offered diets that were standardized within farms, i.e., all cows on a farm were fed on the same diet at any sampling period, and any changes to diet formulation when batches of forage changed were made at least 14 days before sampling commenced. Diets were based on maize silage, grass silage or grass hay, and concentrates in the UK and IT and were based on grass silage and concentrates in SE and FI (table S1). Diets were fed as ad libitum total-mixed rations (TMRs) in IT, SE, and FI and as ad libitum partial-mixed rations (PMRs) plus concentrates during robotic milking in the UK. The PMRs and TMRs were delivered along feed fences in the UK and IT, and TMRs were delivered into individual feed bins in SE and FI.

Milk and body weight recording
Milk yield was recorded at every milking, and daily mean was calculated for each cow. Cows were milked twice daily in herringbone parlors in IT and SE, twice daily at their individual standings in FI, and in automatic milking stations (Lely Astronaut A3, Lely UK Ltd., St. Neots, UK), on average, 2.85 times per day, in the UK.

Milk samples were collected from each cow at four milkings during the sampling period, preserved with Broad Spectrum MicroTabs II containing bronopol and natamycin (D & F Control Systems Inc., San Ramon, CA) or bronopol (Valio Ltd., Finland) and stored at 4°C until analyzed. Milk samples were analyzed for fat, protein, lactose, and urea concentrations using mid-infrared instruments [FOSS MilkoScan (FOSS, Denmark) or similar]. Mean concentrations of milk components were calculated by weighting concentrations proportionally to respective milk yields from evening and morning milkings.

Body weight was recorded three (SE) or two (IT and FI) times during each sampling period and automatically at each milking in the UK. Mean body weight was calculated for each cow.

Feed intake measurement and estimation
Feed intake was recorded individually on a daily basis throughout each sampling period using roughage intake control (RIC) feeders (Insentec B.V., Marknesse, the Netherlands) in SE and manually in FI. Feed intake was estimated using indigestible markers (alkanes) in feed and feces (27) in the UK and IT. Alkanes (C30 and C32) were administered via concentrates fed during milking in the UK and via a bolus gun, while cows were restrained in locking head yokes during feeding in IT. Validation of the alkane method for estimating feed intake was provided by concurrent direct measurement of individual feed intake in 50 cows in the UK via RIC feeders (Fullwood Ltd., Ellesmere, UK) and by applying the method to individually fed cows in a research herd in IT (28).

Collection of rumen samples
The method of sampling rumen fluid was standardized at all centers and involved using a ruminal probe specially designed for cattle (ruminator; profs-products.com). The probe comprises a perforated

brass cylinder attached to a reinforced flexible pipe, a suction pump, and a collection vessel. The brass cylinder was pushed gently to the back of a cow's mouth, and gentle pressure was applied until the device was swallowed as far as a ring on the pipe that indicates correct positioning in the rumen. The first liter of rumen fluid was discarded to avoid saliva contamination, and the next 0.5 liters was retained for sampling. The device was flushed thoroughly with tap water between cows.

Rumen fluid samples were collected on day 1 during the sampling period between 2 and 5 hours after feed was delivered to cows in the morning. For all samples, pH of rumen fluid was recorded immediately. After swirling, four aliquots of 1 ml each were pipetted into freeze-resistant tubes (2-ml capacity), immediately frozen in liquid nitrogen or dry ice, stored at −80°C, and freeze-dried within 1 month from the sampling date. Four additional aliquots of 2.5 ml were pipetted into centrifuge tubes with 0.5 ml of 25% metaphosphoric acid for VFA and ammonia-N analysis, centrifuged at 1000g for 3 min, and the supernatant was transferred to fresh tubes. Tubes were sealed and frozen at −20°C until laboratory analysis.

Rumen VFA measurement
VFA concentrations were determined by gas chromatography using the method of Playne (*29*). Ammonia-N concentration was determined by a photometric test with a Clinical Chemistry Autoanalyzer using an enzymatic ultraviolet method (e.g., Randox Laboratories Ltd., Crumlin, UK).

DNA extraction
Total genomic DNA was isolated from 1 ml of freeze-dried rumen samples according to Yu and Morrison (*30*). This method combines bead beating with the column filtration steps of the QIAamp DNA Stool Mini Kit (Qiagen, Hilden, Germany).

Amplicon sequencing
Primers for polymerase chain reaction (PCR) amplification of bacterial and archaeal 16S rRNA genes, ciliate protozoal 18S rRNA genes, and fungal ITS1 genes were designed in silico using ecoPrimers (*31*), the OBITools software suite (*32*), and a database created from sequences stored in GenBank (table S2). For each sample, PCR amplifications were performed in duplicate. An 8-nucleotide tag unique to each PCR duplicate was attached to the primer sequence to enable the pooling of all PCR products for sequencing and the subsequent assignation of sequence reads to their respective samples. PCR amplicons were combined in equal volumes and purified using a QIAquick PCR purification kit (Qiagen, Germany). After library preparation using a standard protocol with only five PCR cycles, amplicons were sequenced using the MiSeq technology from Illumina (Fasteris, SA, Geneva, Switzerland), which produced 250–base-paired end reads for all markers, except for the archaeal marker, which was sequenced with the HiSeq technology from Illumina, generating 100–base-paired end reads.

Methane and CO$_2$ emission measurement
Methane was measured using breath sampling either during milking in the UK (*33*) or when cows visited a bait station in IT and SE (GreenFeed) (*34*). Methane was measured in FI by housing cows in respiration chambers for 5 days (*35*). Carbon dioxide was measured simultaneously with methane in IT, SE, and FI.

Blood sampling and analysis
Blood samples were collected at the same time as rumen sampling using jugular venipuncture and collection into evacuated tubes (Vacutainer). One tube containing lithium heparin or Na-EDTA as anticoagulant was collected for metabolic parameters, and two tubes containing sodium citrate were collected for genotyping. Tubes were gently inverted 8 to 10 times following collection to ensure optimal additive activity and prevent clotting. Tubes were chilled at 2° to 8°C immediately after collection by placing in chilled water in a fridge or in a mixture of ice and water. Tubes collected for metabolic parameters were centrifuged for 10 to 15 min (3500g at 4°C), and the plasma obtained was divided into four aliquots. Blood samples collected for genotyping were not centrifuged. All samples were stored at −20°C until analyzed.

Plasma non-esterified fatty acids, β-hydroxybutyrate, glucose, albumin, cholesterol, urea, and creatinine were analyzed at each center using commercial kits (Instrumentation Laboratory, Bedford, MA, USA; Wako Chemicals GmbH, Neuss, Germany; and Randox Laboratories Ltd., Crumlin, UK). Blood samples from each center were sent to IT for haptoglobulin determination, according to the method of Skinner *et al.* (*36*).

Quantitative PCR of 16S and 18S rRNA genes
DNA was diluted to 0.1 ng/μl in herring sperm DNA (5 μg/ml) for amplification with universal bacterial primers UniF (GTGSTGCAYGGYYGTCGTCA) and UniR (ACGTCRTCCMCNCCTTCCTC) (*37*) and 1 ng/μl in herring sperm DNA (5 μg/ml) for amplification of other groups (*38*). Quantitative PCR was carried out using a BioRad CFX96 as described by Ramirez-Farias *et al.* (*39*). Amplification of archaeal 16S RNA genes was carried out using the primers Met630f (GGATTAGATACCCSGGTAGT) and Met803r (GTTGARTCCAATTAAACCGCA) as described by Hook *et al.* (*40*) and calibrated using DNA extracted from *Methanobrevibacter smithii* PS, a gift from M. P. Bryant (University of Illinois). For total bacteria amplification, efficiency was evaluated using template DNA from *Roseburia hominis* A2-183 (DSM 16839T). Amplification of protozoal 18S rRNA gene was carried out using primers 316f (GCTTTCGWTGGTAGTGTATT) and 539r (CTTGCCCTCYAATCGTWCT) (*41*) and calibrated using DNA amplified from bovine rumen digesta with primers 54f and 1747r (*41*). Bacterial abundance was calculated from quadruplicate C_t values using the universal bacterial calibration equation.

Bovine genotyping
From blood samples, genomic DNA was extracted and quantified for SNP genotyping. All animals were genotyped on the Bovine GGP HD (GeneSeek Genomic Profilers). The 200 cows coming from FI and SE were genotyped using the Bovine GGP HD chip v1 (80K) that included 76.883 SNPs, while the 800 samples from the UK and IT were genotyped using the Bovine GGP HD chip v2 (150K) that included 138.892 SNPs, as the v1 of the chip was no longer available from the manufacturer. The v2 of the chip includes all the SNPs that were present in the previous v1 of the chip, while, at the same time, providing more markers for the same final processing cost. The Neogen Corporation performed the DNA hybridization, image scanning, and data acquisition of the genotyping chips according to the manufacturer's protocols (Illumina Inc.) All individuals had a call rate higher than 0.90 (93.5% of individuals with call rate higher than 0.99). More than 99% of SNPs had a call rate higher than 0.99 (93.2% of SNPs with call rate higher than 0.99). Minor allele frequency (MAF) distribution evidences more than 90% of markers with a MAF > 5% and nearly 4% of monomorphic SNPs.

Quantification and statistical analysis
Statistical methods and software used are detailed in subsequent sections, figure legends, and Results. Statistical significance was declared at $P < 0.05$, $P < 0.01$, and $P < 0.001$, as appropriate.

Utilization of primer sets derived microbiome data in the statistical analysis

Associations of microbial domain richness were based on amplicon sequencing data from the following primer sets: Bact (bacteria), Arch (archaea), Neoc (fungi), and Cili (protozoa). Associations of individual microbes (as species-level OTUs) were based on amplicon sequencing data from the following primer sets: ProkA (bacteria and archaea), Neoc (fungi), Cili (protozoa).

Converting OBITools intermediate fasta files to QIIME ready format

Amplicon sequences were initially processed with OBITools (32), which removed barcodes and split each sample from each of the two sequencing rounds into an individual FASTQ file. Within each domain's amplicon sequences, individual sample sequences from both rounds were then pooled together into a single FASTQ file in the format required for further processing in QIIME (quantitative insights into microbial ecology) (42) for picking an OTU. In detail, the header of each FASTQ entry was appended with a prefix following the format *[round_id] [sample_id][running_number] [space]*.

Clustering of microbial marker gene amplicon sequences and picking representative de novo species OTU

The marker gene sequences coming from each domain's primer set (Archaea, Bacteria, Prokaryote, Ciliate, protozoa, and Fungi) were clustered using the 97% nucleotide sequence similarity threshold, using the UCLUST algorithm (43), following the QIIME command: *pick_otus.py -m uclust -s 0.97*). Representative OTUs for each OTU cluster were chosen with QIIME command *pick_rep_set.py -m most_abundant*.

Assigning taxonomy to OTU

The OTU within each domain was assigned taxonomy using the Ribosomal Database Project classifier (44), following the QIIME command *assign_taxonomy.py -m rdp*. The OTUs from the amplicon domains of Prokaryotic, Archaea, and Bacteria were assigned taxonomy according to Greengenes database (45). The OTUs from Ciliate protozoa were assigned taxonomy according to the SILVA database; release 123 (46). Fungal OTUs were assigned taxonomy according to a Neocallimastigomycota ITS1 database from Koetschan *et al.* (47).

Creation of OTU tables and sample subsetting and subsampling

Amplicon domain OTU tables were created from the representative OTU set counts in each sample along with their assigned taxonomy, using QIIME command *make_otu_table.py*. Each OTU table was then subsetted to include only the sample from each animal (of the two samples sequenced in two different sequencing rounds) that gained the highest sequence depth. Furthermore, amplicon domain OTU tables were subsampled to a 7000-read depth for all analyses, with the following exceptions: domain richness (8000 reads) and microbe abundance to trait association (8000 reads) and interdomain microbial interaction analysis, where no subsampling was taking place.

Correlating microbial domain cell count

The quantitative PCR–derived microbial counts in each domain were correlated to each other using Spearman *r* correlation using R (48) *cor* function. The *P* values for all interdomain correlations within each farm were corrected using Bonferroni-Hochberg (BH) (49) procedure.

Correlating microbial domain cell counts to experimental variables

Within each farm, each experimental variable was correlated to each microbial domain's cell count (Spearman *r*). Next, the analysis proceeded only with experimental variable—domain count pairs whose correlation direction was identical in all farms. Subsequently, *P* values for the correlation of the selected experimental variable—domain cell count pairs from within each farm were combined by meta-analysis using the weighted sum of *z* procedure (50, 51), weighted by the farm size. Meta-analysis was carried by using R package *metap* (52). Last, combined *P* values were corrected using the BH procedure.

Correlating microbial domain richness to experimental variables

Separately within farms, each experimental variable was correlated to each microbial domain's richness, as observed species count (Spearman *r*), using domain-specific primers. Next, the analysis proceeded only with experimental variable—domain richness pairs whose correlation direction was identical in all farms. Subsequently, *P* values for the correlation of the selected experimental variable—domain richness pairs from within each farm were combined by meta-analysis using the weighted sum of *z* procedure, weighted by the number of cows on each farm.

Meta-analysis was carried by *R* package *metap* (52). Last, combined *P* values were corrected using the BH procedure.

Prediction of phenotypes and other experimental variables by core microbiome

The abundances of the core microbes within each farm were used as features fed into a Ridge regression (19) to predict each of the traits (separately). Our approach followed a *k*-fold cross-validation methodology (*k* = 10), where each fold was omitted once from the entire set and the model built from all the other folds (training set) was used to predict the trait value of the excluded samples (animal). This was implemented using the function *cv.glmnet* (α = 0, *k* = 10) from the GLMNET R package (20). Then, the overall prediction r^2 was calculated using R code *1- model_fit$cvm[which(model_fit$glmnet. fit$lambda == model_fit$lambda.min)] / var(exp_covar)*. Cross-validation procedure was repeated 100 times, and R^2 measurements were averaged.

Prediction of phenotypes by core microbiome while correcting for diet

To estimate the phenotypic variability explained by core microbes with omission of diet components effect, we repeated the analysis above with one difference. That is, before running the regression, both phenotypic values and microbial OTU counts were corrected for diet. In detail, a Ridge regression (19) was used on the basis of diet components as independent variables and the phenotype or OTU as the dependent variable. Thereafter, the phenotype residuals (diet predicted phenotype – actual phenotype) and OTU residuals (diet predicted OTU count – actual OTU count) were used to feed the GLMNET function (20).

Prediction of phenotypes by diet components

Diet components within each farm were used as features fed into a Ridge regression (19) to predict each of the phenotypes (separately). Our approach followed a *k*-fold cross-validation methodology (*k* = 10),

where each fold was omitted once from the entire set and the model built from all the other folds (training set) was used to predict the trait value of the excluded samples (animal). This was implemented using the function *cv.glmnet* (α = 0, *k* = 10) from the GLMNET R package (*20*). Then, the overall prediction r^2 was calculated using *R code 1- model_fit\$cvm[which(model_fit\$glmnet.fit\$lambda == model_fit\$lambda.min)] / var(exp_covar)*. Cross-validation procedure was repeated 100 times, and R^2 measurements were averaged.

Prediction of phenotypes and other experimental variables by core microbiome using RF

As an additional analysis to further verify our findings of core microbiome explainability (by prediction) of host phenotypes and experimental variables, we repeated that analysis using RF regression.

The abundances of the core microbes within each farm were used as features fed into a RF regression model (*21, 22*) to predict each of the traits (separately). Our approach followed a leave-one-out cross-validation methodology where, in each iteration, one sample (animal) was omitted from the entire set, and the model built from all the other animals (training set) was used to predict the trait value of the excluded sample (animal). Thereafter, the prediction R^2 value between vector of actual and predicted values was calculated using R CARET package function R^2.

Bovine genotype quality control

Genotypes of the two breed types were processed independently. Genotypes were first subjected to quality control (QC) filtering including 5% minor frequency allele, 5% genotype missingness, and 5% individual missingness, following PLINK (*53*) command *plink --noweb --cow --maf 0.05 --geno 0.05 --mind 0.05*. The QC for the genotypes used for association/heritability analysis (Holstein excluding farm UK2) resulted with 5377 SNPs failed missingness, 14,119 SNPs failed frequency, and 48 of 635 individuals were removed for low genotyping, resulting with 587 individuals and 121,066 remaining.

Testing association of the global rumen prokaryotic core with host genetics

Within each farm, the first 30 principal components (PCs) for core OTU were extracted (R prcomp). In addition, first genotype PCs were extracted using R *snpgdsPCA* (*54*). Then, CCA (*55*) was performed between the matrices of OTU PCs and genotype PCs, and total fraction of OTU variance accounted for genotype variables through all canonical variates were calculated. This actual value was than compared to that of 1000 random permutations, where the order of phenotype PCs was shuffled.

Creation of genetic relationship matrix

A genetic relatedness matrix (GRM) was created including all Holstein animals except farm UK2, (*56*), using the command *gcta64 --make-grm-bin --make-bed --autosome- num 29 --autosome*.

Heritability estimation

For estimating OTU heritability, the core microbe counts were quantile-normalized and were then provided to genetics complex trait analysis (GCTA) to estimate phenotypic variance explained by all SNPs with genome-based restricted maximum likelihood (GREML) method (*56, 57*), with farms as qualitative covariates and the first five GRM PCs and diet components as quantitative covariates, following the GCTA command *gcta64 --reml –pheno [phenotype_file] –*

mpheno [phneotype_index] --grm --autosome-num 29 –covar [farms_covars_file] --qcovar [quant_covariates_file].

Heritability confidence interval estimation

Heritability confidence intervals at 95% were estimated on the basis of the heritability estimates and the GRM using the GRM eigenvalues and farms as covariates with the program FIESTA (Fast Confidence IntErvals using Stochastic Approximation) (*58*). The command used was *fiesta.py --kinship_eigenvalues [GRM_eigenvalues_file] --kinship_eigenvectors [GRM_eigenvectors_file] --estimates_filename [heritability_estimates_file] --covariates [farms_covariate_file] --confidence 0.95 --iterations 100 --output_filename [otu_file]*.

Bovine genome SNPs—Microbe association effort

Microbial species-level OTU phenotypes within the Holstein subset (excluding the UK2 cohort that showed a different genetic makeup by genotype principal components analysis and ADMIXTURE ancestral background analysis) relative abundance data were transformed using quantile normalization. Moreover, the top five genotype PCs and the farm identity were used as a continuous and categorical covariate, respectively. The analysis was performed with the mixed linear model option (*mlma*) where the SNP under inspection was accounted as fixed effect along with the covariates and GRM effect as random. No association *P* value surpassed the Bonferroni corrected significance threshold (9.076876×10^{-10}) for the number of phenotypes (455) and the number of SNPs included in the association analysis (121,066).

Estimating kinship matrix

Farm wise animal genetic kinship matrices as estimated on the basis of genomic relatedness were inferred from common SNPs that were filtered in after the above quality control procedure. The tool used for the estimation was EMMA expedited (EMMAX)(*59*), with the following command line: *emmax-kin-intel64 -v -M 10 farm_genotypes_tped_file -o farm.hBN.kinf*.

Genomic prediction

Genomic prediction was performed on the basis of each farm's kinship matrix. The genome association and prediction integrated tool (GAPIT) (*60*) tool was used to predict phenotypic values, with the function *GAPIT* (parameters *PCA.total=3, SNP.test=FALSE*). *creareFolds* command from R caret package (*61*) was used to create three folds, where, in each one, fold observations are omitted and are predicted by the model built from the remaining two folds. R^2 is estimated between the observed, and predicted trait values were then correlated using caret R^2 function. The process was repeated 10 times for a given trait in a given farm, and mean of all measurements was then calculated.

Associating microbes' abundance with experimental variables

Separately for each farm and domain, OTUs occupying more than 10% of the animals in that farm were pairwise-correlated (Spearman) to each of the experimental variables. Following that, all *P* values resulted from correlation tests within a given domain and farm were subjected to multiple testing correction using the BH procedure. Last, an OTU that showed a significant correlation (corrected *P* < 0.05) to a certain experimental variable in most (>3) of the farms with same *r* coefficient sign and no significant correlation with opposite *r* sign in the remaining farms was identified as associated with that variable.

Inference of microbial interaction network within domains

Within each domain and farm, an OTU table with a subset of samples (animals) that contain a depth of at least 5000 reads was created, followed by removal of OTUs present in <50% of animals. The raw counts in the OTU table were fed into the R SpiecEasi (Sparse InversE Covariance estimation for Ecological Association and Statistical Inference) (62) framework, and edges were identified using *spiec.easi* function ("mb" method). Edges were given weights using *symBeta* function as suggested by the package authors. Thereafter, the resulting network was filtered to include only edges whose absolute weight was greater than 0.2. Last, all individual farms within a certain domain were merged, and edges connecting nodes (microbes) with the same taxonomic annotation were removed.

Inference of interdomain microbial network

Within each farm, OTUs from different domains were correlated to each other using Spearman correlation, followed by BH correction for all the correlations examined at the farm and filtering in correlations with corrected $P < 0.05$. Then, significant correlations were aggregated from all farms. Last, correlations with correlation coefficient $r < 0.5$ were removed.

Comparing phylogenetic relatedness of core prokaryotic microbes to random sampling

Multiple sequence alignment between all core prokaryotic microbes was calculated using multiple alignment using fast fourier transform (MAFFT) (63, 64) with default parameters. A phylogenetic tree–based distance matrix was obtained from aligned sequences using FastTree (65, 66), following the command *fasttree -nt -makematrix*. Thereafter, the median phylogenetic between core microbes was calculated.

Next, random sets ($n = 100$) of OTU sequences were subjected to the same procedure. The P value was calculated as $P = [I(mcsd > mrsd) +1]/101$, where $mcsd$ represents median core phylogenetic distance and $mrsd$ represents a vector of median phylogenetic distances calculated for the randomly sampled set.

Examining core and trait-related microbiome for taxonomic enrichment

The OR of each prokaryotic order appearing in the examined group (either core microbiome or trait-related microbiome), between the examined group and the whole prokaryotic microbiome catalog, was calculated. Next, orders showing an OR > 1 (higher in the examined group) were filtered in. Last, the OR P value was calculated (Fisher exact test, two-tailed) and corrected using the BH procedure.

Comparing heritable microbes to other core miocrobes' ability to explain experimental variables

To compare the ability of heritable microbes versus other core microbes to explain the experimental variables, we used Ridge regression to fit the heritable microbes as independent variables and the experimental variable as the predictable variable. We then contrasted this R^2 value with other 100 R^2 values achieved from random samples of nonheritable core microbes of same size (39 random microbes). Ridge regression was performed by the R glmnet package. We then compared the R^2 of heritable microbes to the mean R^2 of nonheritable core microbes for all the experimental variables altogether, using a paired Wilcoxon rank-sum test.

Seasonality test

In each farm, core microbes were corrected for diet. Thereafter, the samples in the farm were partitioned into two groups, winter (fall equinox to spring equinox) and summer (spring equinox to fall equinox). Then, each microbial OTU abundance was compared using Wilcoxon rank-sum test that was used to test for the difference between the abundance of the given OTU between the two seasons, followed by a multiple comparison correction using the Bonferroni method. Core microbial OTUs with corrected $P < 0.05$ in at least one farm were considered as showing a seasonal association.

SUPPLEMENTARY MATERIALS

Supplementary material for this article is available at http://advances.sciencemag.org/cgi/content/full/5/7/eaav8391/DC1

Supplementary Materials and Methods

Supplementary Text. Interactions between main categories of ruminal microbes in abundance, diversity, and animal phenotype.

Fig. S1. Rank abundance plot for core microbes along farms.

Fig. S2. Overview of genetic components along the Holstein cohort and host SNP-microbe association effort.

Fig. S3. Microbial species interaction within and between domains.

Fig. S4. Species richness and abundance of rumen microbial domains reveal ecological interactions and connection to host traits.

Fig. S5. Host genetics, core microbiome composition, and diet shape the host phenotypic landscape.

Fig. S6. Heritable microbes tend to explain experimental variables better in comparison to nonheritable core microbes.

Fig. S7. Explained variation (r^2) of different host traits as function of core microbiome composition, according to RF prediction model.

Fig. S8. The vast majority of core microbes do not show a seasonal association, and evidence for seasonality usually does not repeat in more than one farm.

Table S1. Average diet formulations and composition on each farm.

Table S2. Conditions for quantitative PCR.

Data S1. Animals used in the experiment together with diet, measured phenotypes, and other experimental variables.

Data S2. Presence of bacterial taxonomic groups that were found to be most abundant in Henderson *et al.* (6) and appear also in the current study.

Data S3. Presence of archaeal taxonomic groups that were found to be most abundant in Henderson *et al.* (6) and appear also in the present study.

Data S4. Presence of protozoal taxonomic groups that were found to be most abundant in Henderson *et al.* (6) and appear also in the present study.

Data S5. Summary of abundance and occupancy of the core microbial species (prokaryotes, fungi, and protozoa).

Data S6. Heritable microbes.

Data S7. Microbes associated with phenotypic traits.

Data S8. Closest representative sequenced genomes for heritable microbes.

Data S9. Season-affected microbes.

Data S10. Animal genotypes (SNP values).

References (67–70)

REFERENCES AND NOTES

1. H. Steinfeld, P. Gerber, T. Wassenaar, V. Caste, M. Rosales, C. de Haan, *Livestock's Long Shadow* (FAO, 2006).
2. P. R. Myer, T. P. Smith, J. E. Wells, L. A. Kuehn, H. C. I. Freetly, Rumen microbiome from steers differing in feed efficiency. *PLOS ONE* **10**, e0129174 (2015).
3. S. K. Shabat, G. Sasson, A. Doron-Faigenboim, T. Durman, S. Yaacoby, M. E. Berg Miller, B. A. White, N. Shterzer, I. Mizrahi, Specific microbiome-dependent mechanisms underlie the energy harvest efficiency of ruminants. *ISME J.* **10**, 2958–2972 (2016).
4. A. G. Williams, G. S. Coleman, *The Rumen Microbial Ecosystem* (Chapman & Hall, 1997).
5. I. Mizrahi, *The Prokaryotes* (Springer Berlin Heidelberg, 2013).
6. G. Henderson, F. Cox, S. Ganesh, A. Jonker, W. Young; Global Census Collaborators, P. H. Janssen, Rumen microbial community composition varies with diet and host, but a core microbiome is found across a wide geographical range. *Sci. Rep.* **5**, 14567 (2015).
7. C. J. Newbold, G. de la Fuente, A. Belanche, E. Ramos-Morales, N. R. McEwan, The role of ciliate protozoa in the rumen. *Front. Microbiol.* **6**, 1313 (2015).
8. R. J. Gruninger, A. K. Puniya, T. M. Callaghan, J. E. Edwards, N. Youssef, S. S. Dagar, K. Fliegerová, G. W. Griffith, R. Forster, A. Tsang, T. McAllister, M. S. Elshahed, Anaerobic fungi (phylum Neocallimastigomycota): Advances in understanding their taxonomy, life

cycle, ecology, role and biotechnological potential. *FEMS Microbiol. Ecol.* **90**, 1–17 (2014).

9. P. H. Janssen, M. Kirs, Structure of the archaeal community of the rumen. *Appl. Environ. Microbiol.* **74**, 3619–3625 (2008).

10. D. P. Morgavi, E. Rathahao-Paris, M. Popova, J. Boccard, K. F. Nielsen, H. Boudra, Rumen microbial communities influence metabolic phenotypes in lambs. *Front. Microbiol.* **6**, 1060 (2015).

11. B. J. Hayes, K. A. Donoghue, C. M. Reich, B. A. Mason, T. Bird-Gardiner, R. M. Herd, P. F. Arthur, Genomic heritabilities and genomic estimated breeding values for methane traits in Angus cattle. *J. Anim. Sci.* **94**, 902–908 (2016).

12. R. Roehe, R. J. Dewhurst, C. A. Duthie, J. A. Rooke, N. McKain, D. W. Ross, J. J. Hyslop, A. Waterhouse, T. C. Freeman, M. Watson, R. J. Wallace, Bovine host genetic variation influences rumen microbial methane production with best selection criterion for low methane emitting and efficiently feed converting hosts based on metagenomic gene abundance. *PLOS Genet.* **12**, e1005846 (2016).

13. J. A. Rooke, R. J. Wallace, C. A. Duthie, N. McKain, S. M. de Souza, J. J. Hyslop, D. W. Ross, T. Waterhouse, R. Roehe, Hydrogen and methane emissions from beef cattle and their rumen microbial community vary with diet, time after feeding and genotype. *Br. J. Nutr.* **112**, 398–407 (2014).

14. J. K. Goodrich, S. C. Di Rienzi, A. C. Poole, O. Koren, W. A. Walters, J. G. Caporaso, R. Knight, R. E. Ley, Conducting a microbiome study. *Cell* **158**, 250–262 (2014).

15. G. Sasson, S. Kruger Ben-Shabat, E. Seroussi, A. Doron-Faigenboim, N. Shterzer, S. Yaacoby, M. E. Berg Miller, B. A. White, E. Halperin, I. Mizrahi, Heritable bovine rumen bacteria are phylogenetically related and correlated with the cow's capacity to harvest energy from its feed. *MBio* **8**, e00703-17 (2017).

16. A. C. Martiny, K. Treseder, G. Pusch, Phylogenetic conservatism of functional traits in microorganisms. *ISME J.* **7**, 830–838 (2013).

17. J. E. Edwards, N. R. McEwan, A. J. Travis, R. J. Wallace, 16S rDNA library-based analysis of ruminal bacterial diversity. *Antonie Van Leeuwenhoek* **86**, 263–281 (2004).

18. R. J. Wallace, J. A. Rooke, N. McKain, C. A. Duthie, J. J. Hyslop, D. W. Ross, A. Waterhouse, M. Watson, R. Roehe, The rumen microbial metagenome associated with high methane production in cattle. *BMC Genomics* **16**, 839 (2015).

19. D. W. Marquardt, R. D. Snee, Ridge regression in practice. *Am. Stat.* **29**, 3–20 (1975).

20. J. Friedman, T. Hastie, R. Tibshirani, Regularization paths for generalized linear models via coordinate descent. *J. Statist. Software* **33**, 1–22 (2010).

21. A. Liaw, M. Wiener, Classification and regression by randomForest. *R News* **2**, 18–22 (2002).

22. L. Breiman, Random forests. *Mach. Learn.* **45**, 5–32 (2001).

23. D. R. Yáñez-Ruiz, B. Macías, E. Pinloche, C. J. Newbold, The persistence of bacterial and methanogenic archaeal communities residing in the rumen of young lambs. *FEMS Microbiol. Ecol.* **72**, 272–278 (2010).

24. C. Foditsch, R. V. Pereira, E. K. Ganda, M. S. Gomez, E. C. Marques, T. Santin, R. C. Bicalho, Oral administration of *Faecalibacterium prausnitzii* decreased the incidence of severe diarrhea and related mortality rate and increased weight gain in preweaned dairy heifers. *PLOS ONE* **10**, e0145485 (2015).

25. D. R. Yáñez-Ruiz, L. Abecia, C. J. Newbold, Manipulating rumen microbiome and fermentation through interventions during early life: A review. *Front. Microbiol.* **6**, 1133 (2015).

26. P. C. Garnsworthy, J. Craigon, J. Hernandez-Medrano, N. Saunders, On-farm methane measurements during milking correlate with total methane production by individual dairy cows. *J. Dairy Sci.* **95**, 3166–3180 (2012).

27. Y. Unal, P. C. Garnsworthy, Estimation of intake and digestibility of forage-based diets in group-fed dairy cows using alkanes as markers. *J. Agric. Sci.* **133**, 419–425 (1999).

28. P. Bani, F. Piccioli Cappelli, A. Minuti, V. Ficuciello, V. Lopreiato, P. C. Garnsworthy, E. Trevisi, Estimation of dry matter intake by n-alkanes in dairy cows fed TMR: Effect of dosing technique and faecal collection time. *Anim. Prod. Sci.* **54**, 1747–1751 (2014).

29. M. J. Playne, Determination of ethanol, volatile fatty acids, lactic and succinic acids in fermentation liquids by gas chromatography. *J. Sci. Food Agric.* **36**, 638–644 (1985).

30. Z. Yu, M. Morrison, Improved extraction of PCR-quality community DNA from digesta and fecal samples. *Biotechniques* **36**, 808–812 (2004).

31. T. Riaz, W. Shehzad, A. Viari, F. Pompanon, P. Taberlet, E. Coissac, ecoPrimers: Inference of new DNA barcode markers from whole genome sequence analysis. *Nucleic Acids Res.* **39**, e145 (2011).

32. F. Boyer, C. Mercier, A. Bonin, B. Y. Le, P. Taberlet, E. Coissac, obitools: a unix-inspired software package for DNA metabarcoding. *Mol. Ecol. Resour.* **16**, 176–182 (2016).

33. P. C. Garnsworthy, J. Craigon, J. Hernandez-Medrano, N. Saunders, Variation among individual dairy cows in methane measurements made on farm during milking. *J. Dairy Sci.* **95**, 3181–3189 (2012).

34. P. Huhtanen, E. H. Cabezas-Garcia, S. Utsumi, S. Zimmerman, Comparison of methods to determine methane emissions from dairy cows in farm conditions. *J. Dairy Sci.* **98**, 3394–3409 (2015).

35. E. Negussie, J. Lehtinen, P. Mäntysaari, A. R. Bayat, A. E. Liinamo, E. A. Mantysaari, M. H. Lidauer, Non-invasive individual methane measurement in dairy cows. *Animal* **11**, 890–899 (2017).

36. J. G. Skinner, R. A. Brown, L. Roberts, Bovine haptoglobin response in clinically defined field conditions. *Vet. Rec.* **128**, 147–149 (1991).

37. H. Maeda, C. Fujimoto, Y. Haruki, T. Maeda, S. Kokeguchi, M. Petelin, H. Arai, I. Tanimoto, F. Nishimura, S. Takashiba, Quantitative real-time PCR using TaqMan and SYBR Green for *Actinobacillus actinomycetemcomitans*, *Porphyromonas gingivalis*, *Prevotella intermedia*, *tetQ* gene and total bacteria. *FEMS Immunol. Med. Microbiol.* **39**, 81–86 (2003).

38. Z. Fuller, P. Louis, A. Mihajlovski, V. Rungapamestry, B. Ratcliffe, A. J. Duncan, Influence of cabbage processing methods and prebiotic manipulation of colonic microflora on glucosinolate breakdown in man. *Br. J. Nutr.* **98**, 364–372 (2007).

39. C. Ramirez-Farias, K. Slezak, Z. Fuller, A. Duncan, G. Holtrop, P. Louis, Effect of inulin on the human gut microbiota: stimulation of *Bifidobacterium adolescentis* and *Faecalibacterium prausnitzii*. *Br. J. Nutr.* **101**, 541–550 (2009).

40. S. E. Hook, K. S. Northwood, A.-D. G. Wright, B. W. McBride, Long-term monensin supplementation does not significantly affect the quantity or diversity of methanogens in the rumen of the lactating dairy cow. *Appl. Environ. Microbiol.* **75**, 374–380 (2009).

41. J. T. Sylvester, S. K. R. Karnati, Z. Yu, M. Morrison, J. L. Firkins, Development of an assay to quantify rumen ciliate protozoal biomass in cows using real-time PCR. *J. Nutr.* **134**, 3378–3384 (2004).

42. J. G. Caporaso, J. Kuczynski, J. Stombaugh, K. Bittinger, F. D. Bushman, E. K. Costello, N. Fierer, A. G. Peña, J. K. Goodrich, J. I. Gordon, G. A. Huttley, S. T. Kelley, D. Knights, J. E. Koenig, R. E. Ley, C. A. Lozupone, D. McDonald, B. D. Muegge, M. Pirrung, J. Reeder, J. R. Sevinsky, P. J. Turnbaugh, W. A. Walters, J. Widmann, T. Yatsunenko, J. Zaneveld, R. Knight, QIIME allows analysis of high-throughput community sequencing data. *Nat. Methods* **7**, 335–336 (2010).

43. R. C. Edgar, Search and clustering orders of magnitude faster than BLAST. *Bioinformatics* **26**, 2460–2461 (2010).

44. J. R. Cole, Q. Wang, J. A. Fish, B. Chai, D. M. McGarrell, Y. Sun, C. T. Brown, A. Porras-Alfaro, C. R. Kuske, J. M. Tiedje, Ribosomal Database Project: data and tools for high throughput rRNA analysis. *Nucleic Acids Res.* **42**, D633–D642 (2014).

45. T. Z. DeSantis, P. Hugenholtz, N. Larsen, M. Rojas, E. L. Brodie, K. Keller, T. Huber, D. Dalevi, P. Hu, G. L. Andersen, Greengenes, a chimera-checked 16S rRNA gene database and workbench compatible with ARB. *Appl. Environ. Microbiol.* **72**, 5069–5072 (2006).

46. C. Quast, E. Pruesse, P. Yilmaz, J. Gerken, T. Schweer, P. Yarza, J. Peplies, F. O. Glockner, The SILVA ribosomal RNA gene database project: improved data processing and web-based tools. *Nucleic Acids Res.* **41**, D590–D596 (2012).

47. C. Koetschan, S. Kittelmann, J. Lu, T. Al-Halbouni, G. N. Jarvis, T. Muller, M. Wolf, P. H. Janssen, Internal transcribed spacer 1 secondary structure analysis reveals a common core throughout the anaerobic fungi (Neocallimastigomycota). *PloS One* **9**, e91928 (2014).

48. R Core Team R: A Language and Environment for Statistical Comput. Secur. (2015).

49. Y. Benjamini, Y. Hochberg, Controlling the false discovery rate: A practical and powerful approach to multiple testing. *J. R. Stat. Soc. Series B* **57**, 289–300 (1995).

50. D. V. Zaykin, Optimally weighted Z-test is a powerful method for combining probabilities in meta-analysis. *J. Evol. Biol.* **24**, 1836–1841 (2011).

51. R. Rosenthal, Combining results of independent studies. *Psychol. Bull.* **85**, 185–193 (1978).

52. M. Dewey, Metap: meta-analysis of significance values. R package version 1.0 (2018).

53. S. Purcell, B. Neale, K. Todd-Brown, L. Thomas, M. A. R. Ferreira, D. Bender, J. Maller, P. Sklar, P. I. W. de Bakker, M. J. Daly, P. C. Sham, PLINK: A tool set for whole-genome association and population-based linkage analyses. *Am. J. Hum. Genet.* **81**, 559–575 (2007).

54. X. Zheng, snpgdsGRM: Genetic Relationship Matrix (GRM) for SNP genotype data. In "SNPRelate: Parallel Computing Toolset for Relatedness and Principal Component Analysis of SNP Data" Version 1.14.0

55. C. T. Butts, yacca: Yet Another Canonical Correlation Analysis Package. R package version 1.1.1 (2018); https://CRAN.R-project.org/package=yacca

56. J. Yang, S. H. Lee, M. E. Goddard, P. M. Visscher, GCTA: A tool for genome-wide complex trait analysis. *Am. J. Hum. Genet.* **88**, 76–82 (2011).

57. J. Yang, B. Benyamin, B. P. McEvoy, S. Gordon, A. K. Henders, D. R. Nyholt, P. A. Madden, A. C. Heath, N. G. Martin, G. W. Montgomery, M. E. Goddard, P. M. Visscher, Common SNPs explain a large proportion of the heritability for human height. *Nat. Genet.* **42**, 565–569 (2010).

58. R. Schweiger, E. Fisher, E. Rahmani, L. Shenhav, S. Rosset, E. Halperin, Using stochastic approximation techniques to efficiently construct confidence intervals for heritability. *J. Comput. Biol.* **25**, 794–808 (2018).

59. H. M. Kang, J. H. Sul, S. K. Service, N. A. Zaitlen, S.-y. Kong, N. B. Freimer, C. Sabatti, E. Eskin, Variance component model to account for sample structure in genome-wide association studies. *Nat. Genet.* **42**, 348–354 (2010).

60. A. E. Lipka, F. Tian, Q. Wang, J. Peiffer, M. Li, P. J. Bradbury, M. A. Gore, E. S. Buckler, Z. Zhang, GAPIT: genome association and prediction integrated tool. *Bioinformatics* **28**, 2397–2399 (2012).

61. Max Kuhn. Contributions from Jed Wing, Steve Weston, Andre Williams, Chris Keefer, Allan Engelhardt, Tony Cooper, Zachary Mayer, Brenton Kenkel, the R Core Team, Michael Benesty, Reynald Lescarbeau, Andrew Ziem, Luca Scrucca, Yuan Tang, Can Candan and Tyler Hunt. (2018). caret: Classification and Regression Training. *R* package version 6.0-80. https://CRAN.R-project.org/package=caret

62. Z. D. Kurtz, C. L. Muller, E. R. Miraldi, D. R. Littman, M. J. Blaser, R. A. Bonneau, Sparse and compositionally robust inference of microbial ecological networks. *PLOS Comput. Biol.* **11**, e1004226 (2015).

63. K. Katoh, K. Misawa, K.-i. Kuma, T. Miyata, MAFFT: A novel method for rapid multiple sequence alignment based on fast Fourier transform. *Nucleic Acids Res.* **30**, 3059–3066 (2002).

64. K. Katoh, D. M. Standley, MAFFT multiple sequence alignment software version 7: improvements in performance and usability. *Mol. Biol. Evol.* **30**, 772–780 (2013).

65. M. N. Price, P. S. Dehal, A. P. Arkin, FastTree: Computing large minimum evolution trees with profiles instead of a distance matrix. *Mol. Biol. Evol.* **26**, 1641–1650 (2009).

66. M. N. Price, P. S. Dehal, A. P. Arkin, FastTree 2–approximately maximum-likelihood trees for large alignments. *PLOS ONE* **5**, e9490 (2010).

67. R. J. Wallace, C. A. McPherson, Factors affecting the rate of breakdown of bacterial protein in rumen fluid. *Br. J. Nutr.* **58**, 313–323 (1987).

68. R. A. Leng, J. V. Nolan, Nitrogen metabolism in the rumen. *J. Dairy Sci.* **67**, 1072–1089 (1984).

69. C. J. Newbold, K. Hillman, The effect of ciliate protozoa on the turnover of bacterial and fungal protien in the rumen of sheep. *Lett. Appl. Microbiol.* **11**, 100–102 (1990).

70. I. Tapio, T. J. Snelling, F. Strozzi, R. J. Wallace, The ruminal microbiome associated with methane emissions from ruminant livestock. *J. Anim. Sci. Biotechnol.* **8**, 7 (2017).

Science Advances

A heritable subset of the core rumen microbiome dictates dairy cow productivity and emissions

R. John Wallace, Goor Sasson, Philip C. Garnsworthy, Ilma Tapio, Emma Gregson, Paolo Bani, Pekka Huhtanen, Ali R. Bayat, Francesco Strozzi, Filippo Biscarini, Timothy J. Snelling, Neil Saunders, Sarah L. Potterton, James Craigon, Andrea Minuti, Erminio Trevisi, Maria L. Callegari, Fiorenzo Piccioli Cappelli, Edward H. Cabezas-Garcia, Johanna Vilkki, Cesar Pinares-Patino, Katerina O. Fliegerová, Jakub Mrázek, Hana Sechovcová, Jan Kopecný, Aurélie Bonin, Frédéric Boyer, Pierre Taberlet, Fotini Kokou, Eran Halperin, John L. Williams, Kevin J. Shingfield and Itzhak Mizrahi

ARTICLE TOOLS	http://advances.sciencemag.org/content/5/7/eaav8391
SUPPLEMENTARY MATERIALS	http://advances.sciencemag.org/content/suppl/2019/07/01/5.7.eaav8391.DC1
REFERENCES	This article cites 62 articles, 6 of which you can access for free http://advances.sciencemag.org/content/5/7/eaav8391#BIBL
PERMISSIONS	http://www.sciencemag.org/help/reprints-and-permissions

Use of this article is subject to the Terms of Service